The CARMENES search for exoplanets around M dwarfs

Line-by-line sensitivity to activity in M dwarfs

Marina Lafarga Magro (she/her)
marina.lafarga-magro@warwick.ac.uk

M. Lafarga, I. Ribas, M. Zechmeister, A. Reiners, Á. López-Gallifa, D. Montes, A. Quirrenbach, P. J. Amado, J. A. Caballero, M. Azzaro, V. J. S. Béjar, A. P. Hatzes, Th. Henning, S. V. Jeffers, A. Kaminski, M. Kürster, P. Schöfer, A. Schweitzer, H. M. Tabernero, M. R. Zapatero Osorio

arXiv: 2302.04794

1. Context

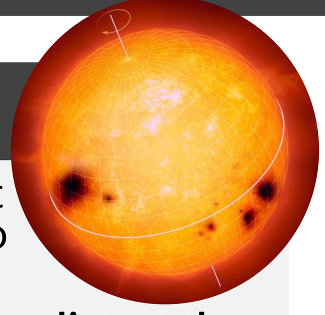

- Radial velocities (RVs) measured from the shift of stellar absorption lines are routinely used to study exoplanets.
- **Stellar activity** features such as spots or faculae **distort the line profiles**, challenging exoplanet studies.
- Absorption **lines** are created by several species, which are **non-uniformly affected by stellar activity.**
- Several works are now focusing on activity effects on a **line-by-line** (LBL) basis [e.g. **1-8**], as opposed to classical methods to measure RVs, which *average* all lines.

2. Goal

Study how spectral lines in M dwarfs are independently impacted by stellar activity.

! Note: We use the word *lines* to refer to minima in the spectrum, even though these features are not true atomic lines but blends of several lines or a feature in a molecular band.

3. Data

CARMENES optical spectra of several very active M dwarfs

- 520–960 nm, R = 94600 [**9**]
- 6 early- and mid-type M dwarfs
- pEWHα ~ −2 to −7
- Rotational velocity < 7 km/s
- Activity-dominated RVs (scatter > 20 m/s)

4. Methods

- Select lines in a high S/N template [as in **10**].
- Compute **RV** time series **for each line**.
- Compute **correlation between line RV & activity indicators.** Use Pearson's correlation coefficient R to assess the correlation strength.
- Select lines with a weak correlation (R~0, i.e. *activity-insensitive* lines) and use those lines to recompute global RVs.

5. Results

Figure examples for YZ CMi (J07446+035) and EV Lac (J22468+443)

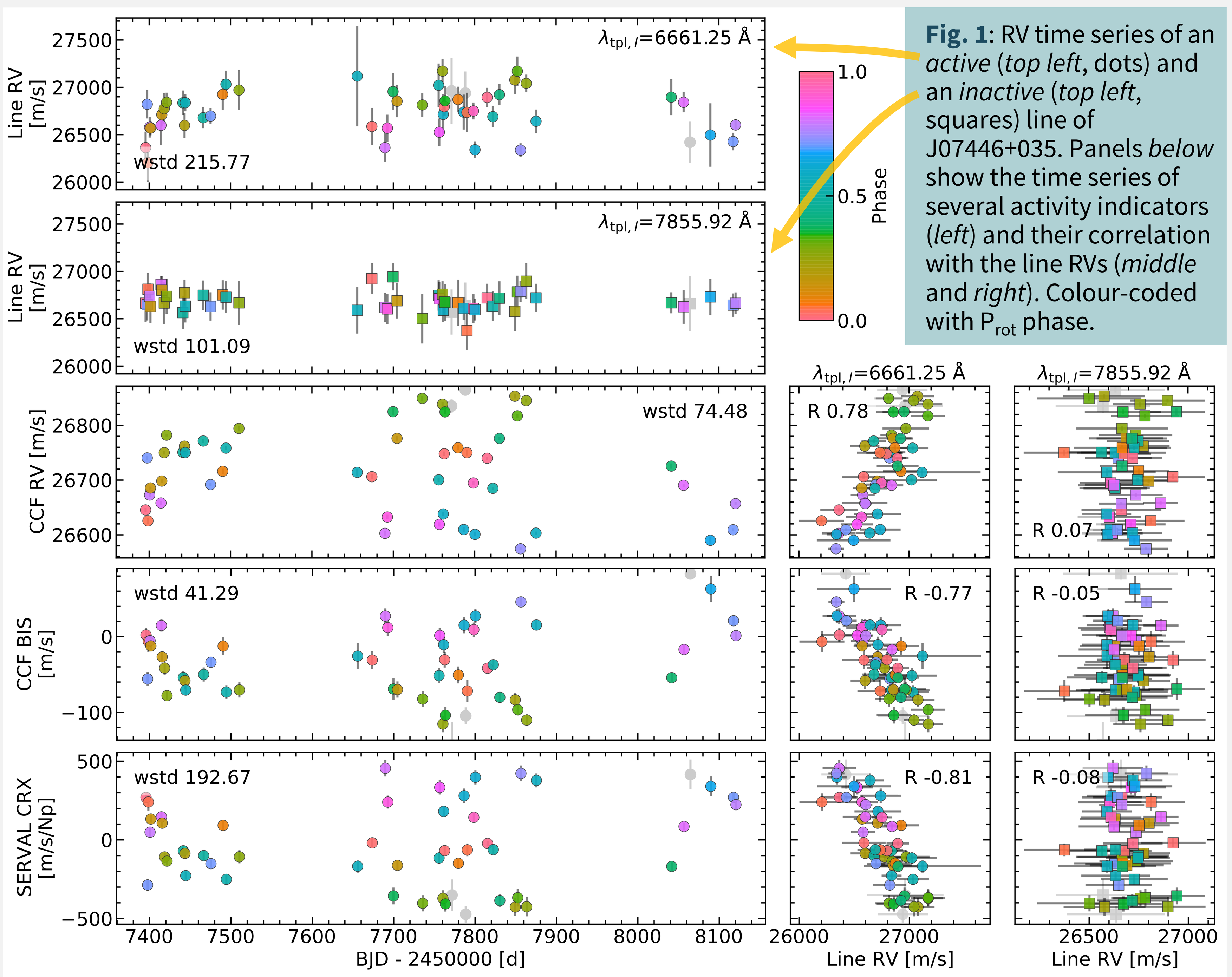

Fig. 1: RV time series of an *active* (*top left*, dots) and an *inactive* (*top left*, squares) line of J07446+035. Panels *below* show the time series of several activity indicators (*left*) and their correlation with the line RVs (*middle* and *right*). Colour-coded with P_{rot} phase.

- The correlations allow us to **classify lines with different sensitivities to activity** in 5 stars (see an example of two lines in **Fig. 1**).
- By using activity-insensitive lines in the global RV calculation we **decrease the global RV scatter** from 2 to 5 times, as well as **decrease the significance of the periodogram peak at the stellar rotation period** P_{rot} (**Fig. 2**).
- The same **lines in similar stars** do **not** show the exact **same sensitivity** to activity (**Fig. 3**).

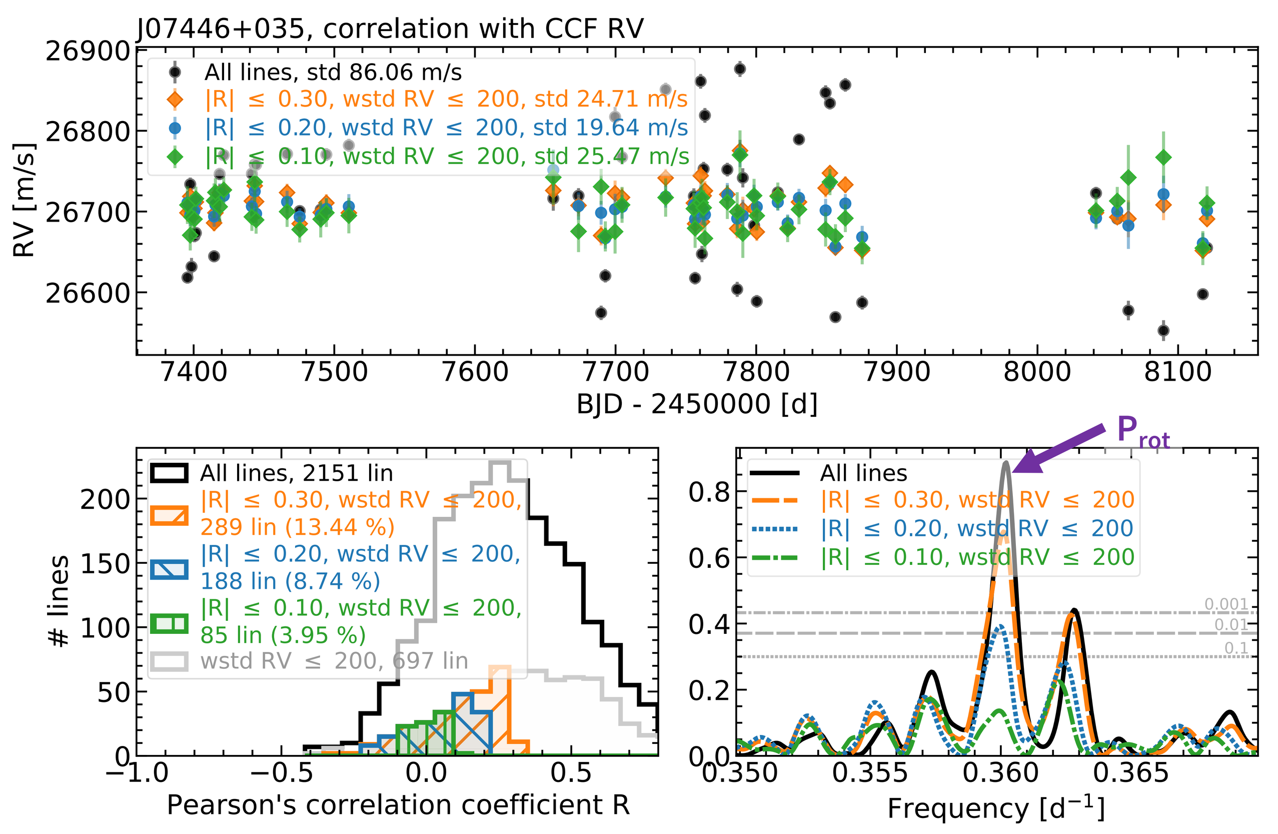

Fig. 2: Decrease of the activity signal using inactive lines. *Top*: RV time series for 3 subsets of inactive lines (colours) and all lines (black), scatter in legend. *Bottom left*: Distribution of R values for all lines and selected subsets. *Bottom right*: Periodogram of the RVs close to P_{rot}.

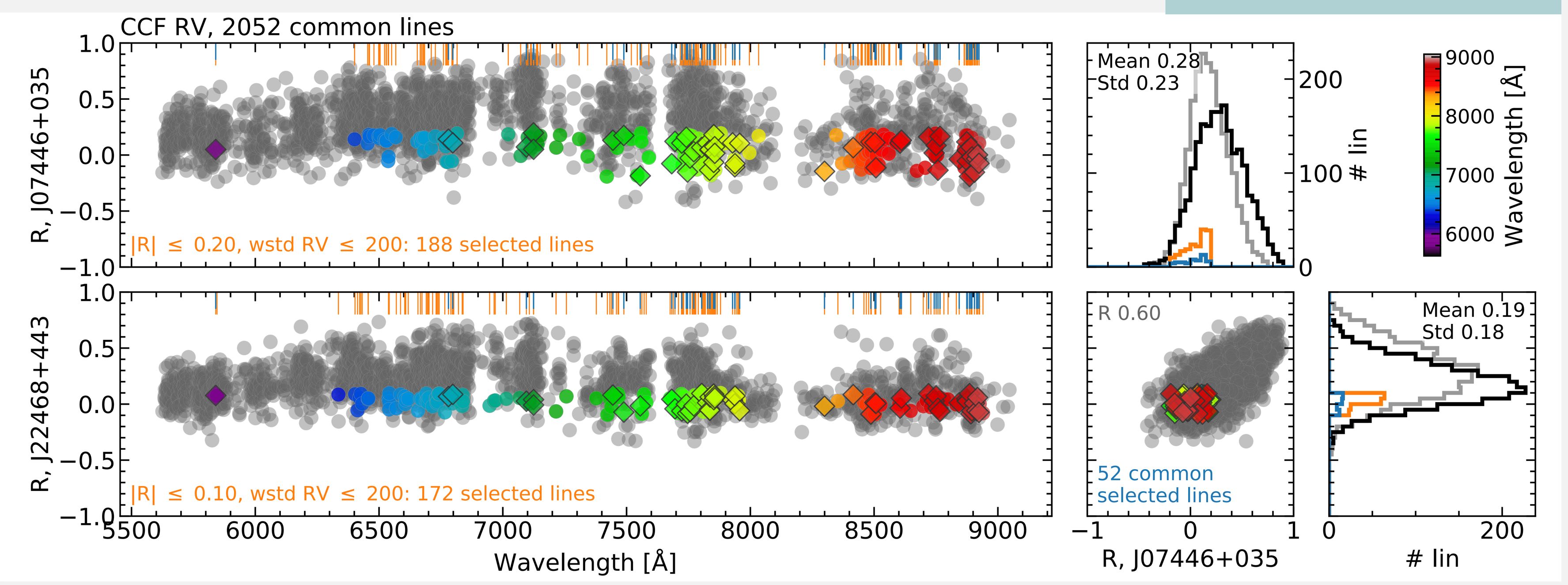

Fig. 3: Comparison of the R values of two stars. Coloured dots show inactive lines, and coloured diamonds show inactive lines common for both stars.

6. Conclusions

- LBL RVs from (active) M dwarf spectra are sensitive to activity to varying degrees.
- By selecting activity-insensitive lines we can mitigate activity effects in RVs.
- Activity effects vary in the same insensitive lines from star to star, making a generalisation of insensitive lines challenging.
- This work can be expanded in many ways!
  - Line (and global) RV computation
  - Correlation quantification and line selection
  - Line physical parameters

The hot Neptune WASP-166 b with ESPRESSO III

A blue-shifted tentative water signal constrains the presence of clouds

M. Lafarga, M. Brogi, S. Gandhi, H. M. Cegla, J. V. Seidel, L. Doyle, R. Allart, N. Buchschacher, M. Lendl, C. Lovis, D. Sosnowska

arXiv: 2302.07916

1. System

A bloated super-Neptune in the hot Neptunian desert [**11**]

WASP-166

- V ~ 9 mag
- Spectral type F9 V
- T_{eff} = 6050 K
- vsini ~ 5 km/s
- M_s = 1.19 M_{Sun}

WASP-166 b

- M_p = 0.102 M_{Jup}
- R_p = 0.63 R_{Jup}
- T_{eq} = 1270 K
- P_{orb} = 5.4 d (0.06 AU)

2. Goal

Constrain the presence of **H_2O** and **clouds** in WASP-166 b using **high-resolution cross-correlation spectroscopy** (HRCCS).

3. Data

2 ESPRESSO transits

- 378–789 nm, R = 140000 [**12**]
- Observations used to model the stellar surface with the Rossiter-McLaughlin [**13**] & confirm the presence of planetary Na [**14**].

4. Methods

- Correct spectra for **tellurics** with a principal component analysis (**PCA**) [**15**].
- Compute the **cross-correlation** (CC) of the processed spectra with a **grid of H_2O models** with different **H_2O abundances** and **cloud deck pressures** [**16**].
- Use the **CC-to-logLikelihood framework** [17,18] to combine orders & nights and assess detection significance.

5. Results & conclusions

PCA optimisation

- Implement an improved PCA algorithm in which we **selectively feed telluric lines**, rather than using the whole spectral range as is standard (**Fig. 1**).

→ **Improve telluric removal** with respect to a standard PCA.

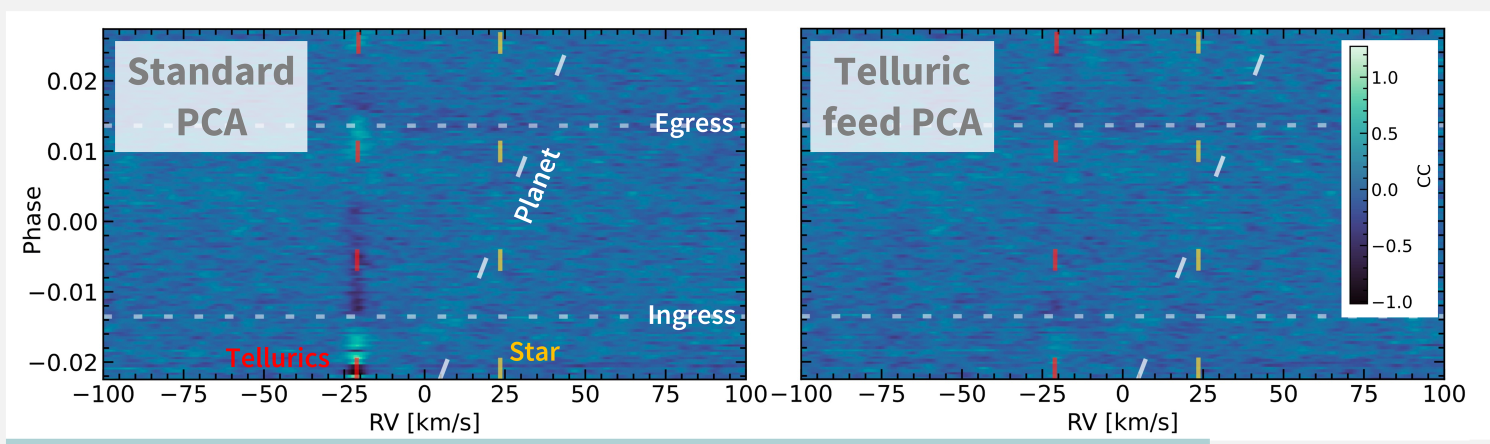

Fig. 1: CCFs (colour) of the 1st night, as a function of orbital phase (y-axis), where the x-axis is the CCF RV grid. *Left* with standard PCA, and *right*, with our improved PCA.

Model comparison

- Models with high H_2O abundance & high cloud pressure are strongly **rejected**, as well as models with low H_2O abundance & low cloud pressure (**Fig. 2**).
- The **preferred models** have **intermediate abundances & pressures.**

→ H_2O detection? **If no H_2O was present, the preferred models would be those compatible with a flat spectrum** (i.e. low abundance & low pressure), which is not seen here.

A tentative H_2O signal from WASP-166 b?

- **Blueshifted** (~5 km/s) **signal** close to the expected planet RV (**Fig. 3**).
- Blueshift could be due to the presence of winds [**14**].

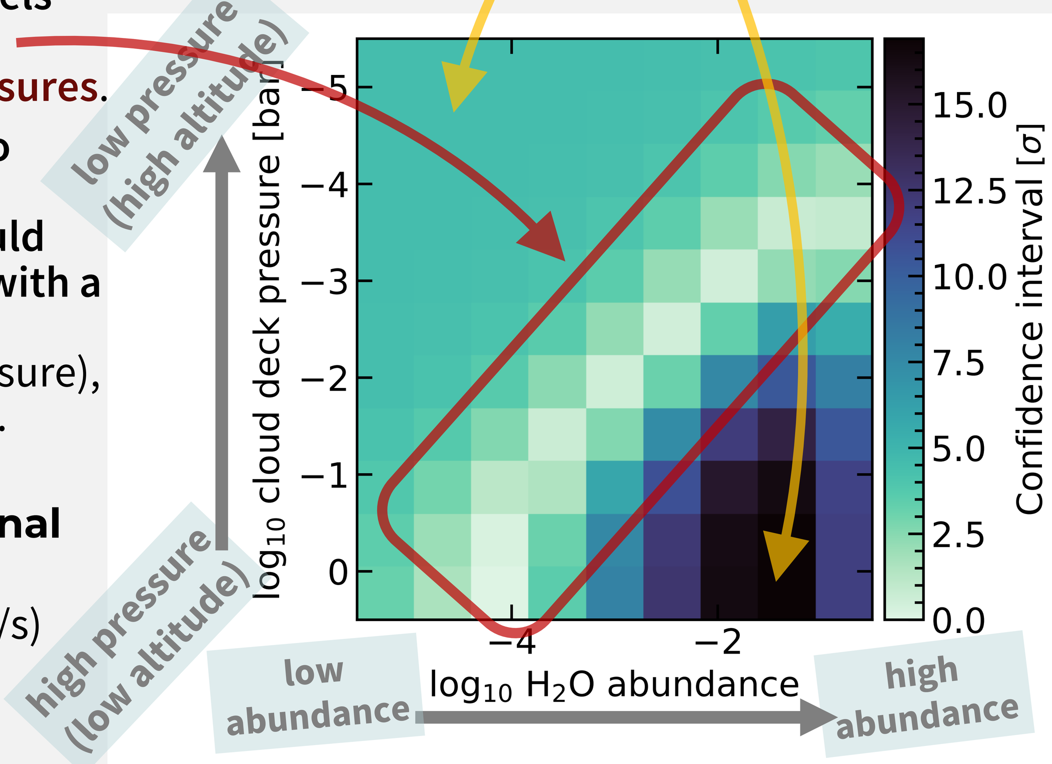

Fig. 2: Confidence intervals (colour) for the grid of models with H_2O abundances ($log_{10}(H_2O)$ = −1 to −5 VMR, x-axis) & cloud deck pressures ($log_{10}(P)$ = 0 to −5 bar, y-axis). Both nights.

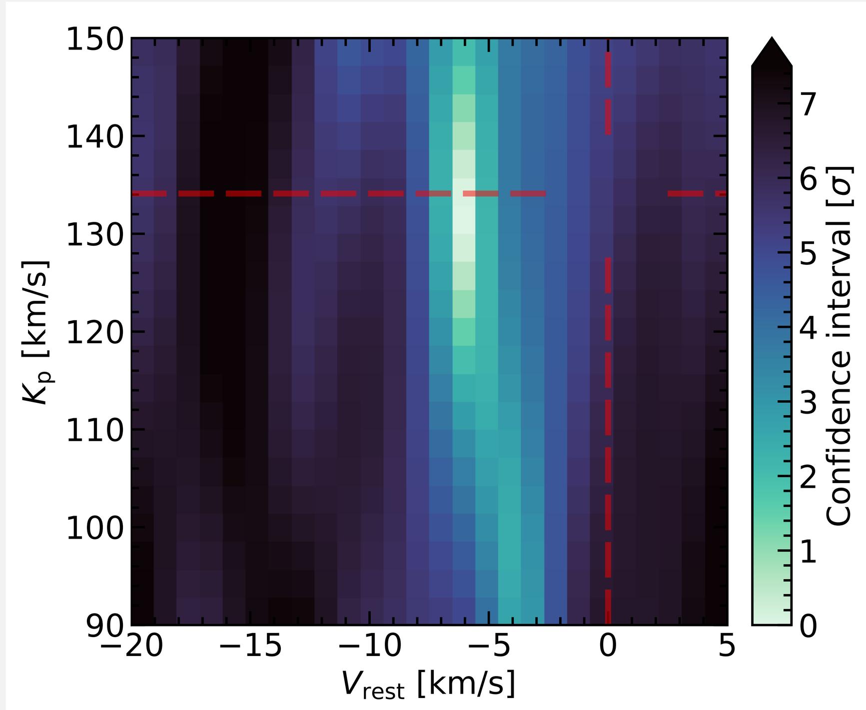

Fig. 3: K_p–V_{rest} confidence interval map (colour) obtained with the preferred model ($log_{10}(H_2O)$ = −4 & $log_{10}(P)$ = 0 bar). Red dashed lines show the expected K_p and V_{rest}. Both nights.

References

[1] Davis et al. 2017
[2] Thompson et al. 2017
[3] Dumusque 2018
[4] Wise et al. 2018
[5] Cretignier et al. 2020
[6] Siegel et al. 2022
[7] Bellotti et al. 2022
[8] Artigau et al. 2022
[9] Quirrenbach et al. 2016
[10] Lafarga et al. 2020
[11] Hellier et al. 2019
[12] Pepe et al. 2021
[13] Doyle et al. 2022
[14] Seidel et al. 2022
[15] Giacobbe et al. 2021
[16] Gandhi et al. 2020 b
[17] Brogi & Line 2019
[18] Gibson et al. 2020

Based on observations made with ESO (programme ID 106.21EM) and CAHA telescopes. Funding from a UKRI Future Leader Fellowship (MR/S035214/1).

WARWICK THE UNIVERSITY OF WARWICK
Institute of Space Sciences
CSIC IEEC